Pancreatic metastasis from papillary thyroid carcinoma: Case report and literature review

Rachel Stein[1] **DO,**
Taylor S. Harmon[1] **MD,**
Caitlin E. Harmon[2]**,**
Enoch Kuo[3] **MD,**
Savas Ozdemir[1] **MD**

1. University of Florida School of Medicine, Jacksonville
2. University of the Incarnate Word School of Osteopathic Medicine
3. University of Florida School of Medicine

Keywords: Papillary thyroid cancer - Pancreatic metastases - PET/CT - SPECT/CT

Corresponding author:
Rachel Stein DO
University of Florida School of Medicine, Jacksonville
655 West 8th Street, C90
2nd Floor, Clinical Center
Jacksonville, FL 32209
904-244-4298
rachel.stein@jax.ufl.edu

Received:
16 March 2021
Accepted revised:
31 May 2021

Abstract
Papillary thyroid carcinoma (PTC) is the most common type of thyroid malignancy. Papillary thyroid carcinoma generally spreads locally to the cervical lymph nodes, but distant metastases are seen in 5%-7% of cases. Most distant metastases occur in the bone, lung, and brain. Pancreatic metastases of PTC are extremely rare. Herein we present a patient with PTC treated with total thyroidectomy and two rounds of radioactive iodine (RAI) ablation that was subsequently found to have a pancreatic metastasis detected on fluorine-18-fluorodeoxyglucose positron emission tomography/computed tomography (^{18}F-FDG PET/CT) imaging 3 years from the initial diagnosis.

Hell J Nucl Med 2020; 24(2): 140-148 *Epub ahead of print: 6 August 2021* *Published online: 27 August 2021*

Introduction

Differentiated thyroid carcinoma is the most common thyroid malignancy and is further classified into papillary and follicular thyroid carcinomas[1]. Papillary thyroid carcinoma (PTC) has an excellent prognosis with a 5-year relative survival rate of 98% [2]. Classical PTC is the most common histological subtype; however, there are several aggressive variants including tall cell, columnar cell, and hobnail variants, with the tall cell variant being the most common [3]. Generally, PTC recurs locally in the cervical lymph nodes with distant metastases only occurring within 5%-7% of cases [4]. Most common sites of metastases are to the bone, lung, and brain, respectively [5]. Pancreatic metastases of PTC are exceptionally rare with only 17 cases reported in the literature [4-20]. Imaging of pancreatic metastases is a diagnostic dilemma as metastases often have similar imaging characteristics to primary pancreatic cancers[4].

We present a case of papillary thyroid carcinoma found to have a pancreatic metastasis 3 years after initial diagnosis on follow-up fluorine-18-fluorodeoxyglucose positron emission tomography/computed tomography (^{18}F-FDG PET/CT). Highlighted are specific imaging characteristics found in this patient population.

Case presentation

A 46-year-old male without any significant past medical history presented for outpatient work-up of a progressively enlarging neck mass and shortness of breath for the past four months. A contrast enhanced axial CT of the cervical soft tissues demonstrated a large thyroid mass with extension into the mediastinum, paravertebral space, and left tracheoesophageal region. There was severe narrowing of the airway within this region (Figure 1).

The patient underwent total thyroidectomy, where tumor invasion was identified within the left recurrent laryngeal nerve, trachea, and esophagus. The surgical pathology specimen returned demonstrating invasive tall-cell variant of papillary carcinoma of the thyroid demonstrating cervical lymph nodal invasion and positive posterior margin. Following resection, the patient was referred to nuclear medicine for radioactive iodine (RAI) ablation. A pre-ablation whole body iodine-123 (^{123}I) scan and single photon emission computed tomography/computed tomography (SPECT/CT) demonstrated residual thyroid tissue and neoplasm that was left during surgery (Figure 2).

The patient received 200mCi of iodine-131 (^{131}I).Thyroglobulin (Tg) was 270.1ng/mL (reference range 2.8-40.9ng/mL) and Thyroglobulin antibodies (TgAb) were <1IU/mL (reference range < or =1IU/mL) at time of RAI ablation.Follow-up post-ablation whole body ^{131}I scan and ^{18}F-FDG SPECT/CT were performed (Figure 3).

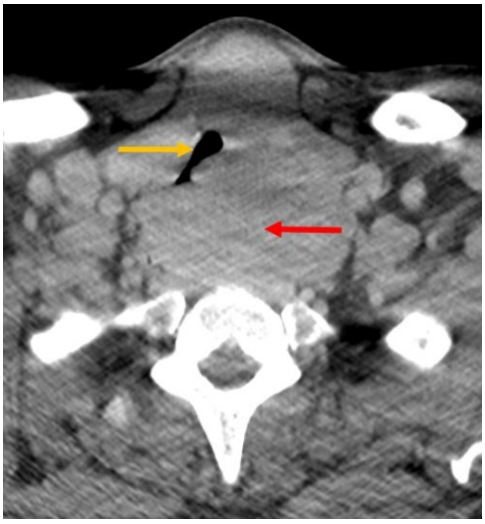

Figure 1. Contrast enhanced axial CT of the cervical soft tissues shows a large thyroid mass with extension into the mediastinum, paravertebral space, and left tracheoesophageal region (red arrow), with severe narrowing of trachea (orange arrow).

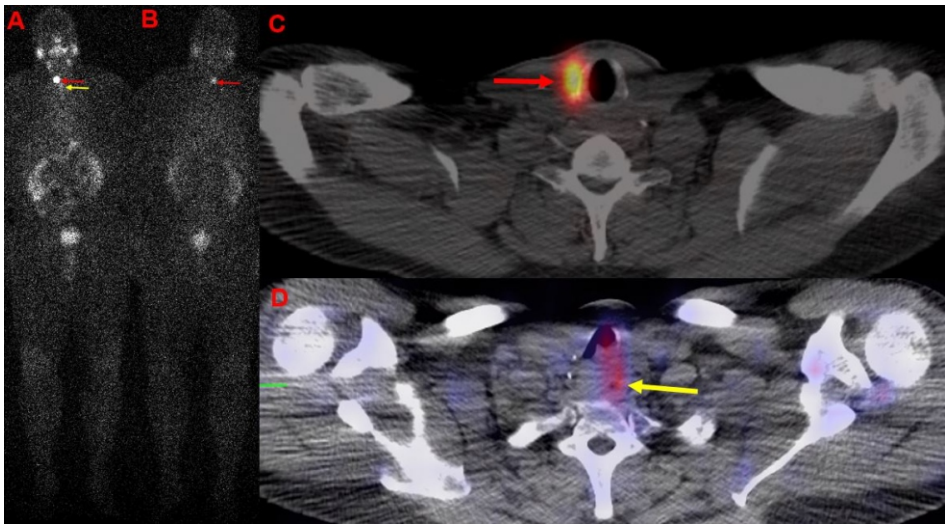

Figure 2. (A&B) Anterior and posterior pre-ablation whole body ^{123}I scan and (C&D) axial fused SPECT/CT images of the neck shows increased uptake in the region of the right thyroid lobe, most consistent with residual thyroid tissue (red arrow). There is a subtle focal area of increased uptake inferiorly on the left, which likely represent known neoplasm left during surgery (yellow arrow).

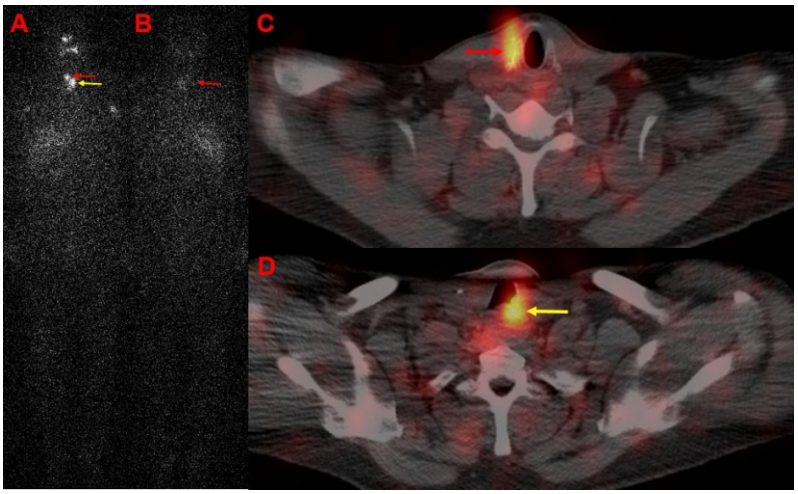

Figure 3. (A&B) Anterior and posterior post-ablation whole body ^{131}I scan and (C&D) axial fused SPECT/CT images of the neck redemonstrate increased uptake in the region of the right thyroid lobe (red arrow), most consistent with post-surgical residual thyroid tissue. Previously seen focal area of increased uptake inferiorly on the pre-ablation ^{123}I scan is much more conspicuous with neoplasm left during surgery (yellow arrow).

Four months after RAI ablation, the patient returned to the emergency department with shortness of breath. A repeat contrast CT of the cervical soft tissues revealed recurrent thyroid neoplasm, and the patient was intubated for airway protection. During that admission, the patient was extubated and a tracheostomy was placed (Figure 4).

The patient was discharged home with the tracheostomy and received outpatient thyroid radiation therapy. Unfortunately, the patient developed radiation induced strictures within the esophagus, and a tracheoesophageal fistula, requiring endoscopic placement of a gastrojejunostomy tube for enteral nutrition. One month after tracheostomy placement, a second pre-ablation ^{123}I whole body scan, followed by another round of 200mCi ^{131}I RAI ablation were performed (Figure 5). After the second RAI, the patient received 70 Gray (Gy) at 2Gy/fractions external beam radiotherapy to the high-risk target volume of the residual thyroid lesion.

One year later, the incurrent development of an ^{18}F-FDG avid pancreatic mass was identified, in addition to the presence of persistent residual/recurrent thyroid neoplasm, on a surveillance ^{18}F-FDG PET/CT from an outside hospital (Figure 6).

The patient was taken for surgical resection of the pancreatic head mass, and surgical histopathological analysis was performed. Histopathological analysis revealed a well-circumscribed, friable, hemorrhagic mass upon gross examination, measuring 3.0cm in the greatest dimension. The mass showed a papillary architecture with well-visualized fibrovascular cores lined by a single layer of cuboidal cells with eosinophilic cytoplasm. The specimen cells demonstrated scattered atypical mitotic figures, prominent nucleoli, and nuclear grooves. Rare nuclear pseudoinclusions were also

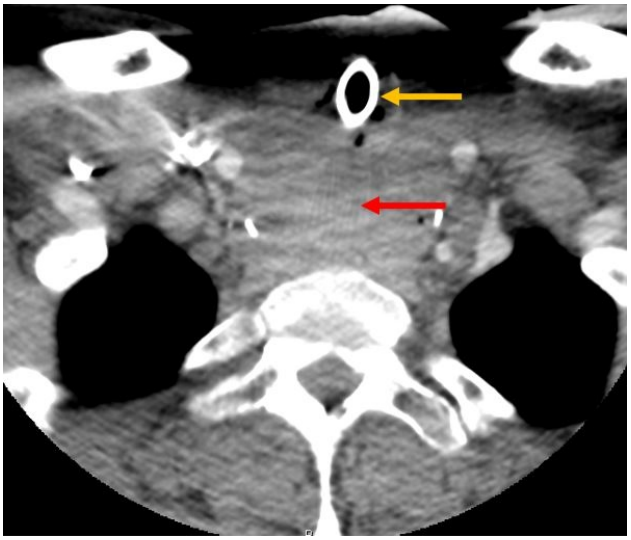

Figure 4. Axial contrast enhanced CT shows recurrent thyroid neoplasm (red arrow). A tracheostomy (orange arrow) was placed, and can be seen within the airway.

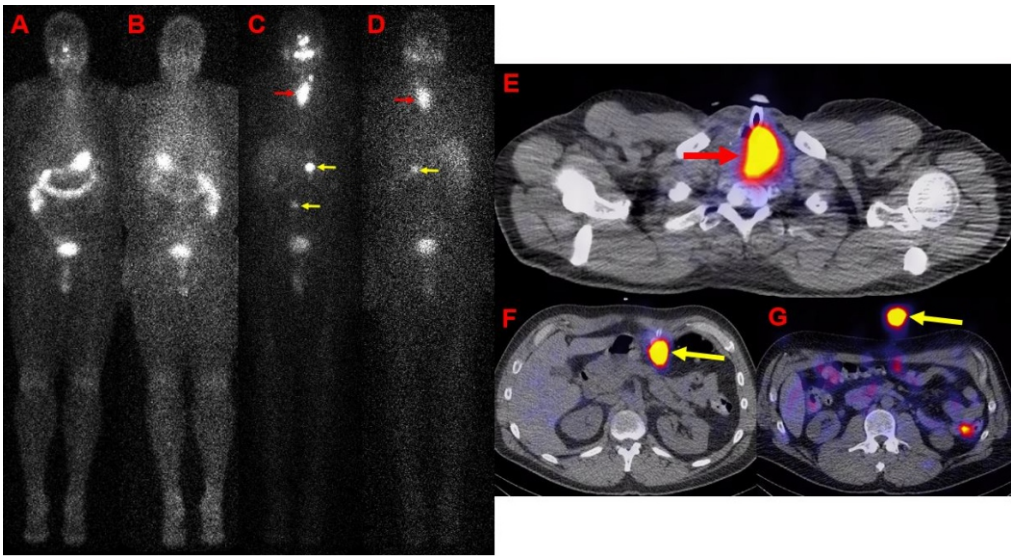

Figure 5. Prior to second ^{131}I treatment, (A&B) anterior and posterior pre-ablation whole body ^{123}I scan and (C&D) anterior and posterior post-ablation whole body ^{131}I scans followed by (E-G) axial fused SPECT/CT images show significant increased radiotracer uptake in the thyroid bed on post-ablation images (red arrows), concerning for recurrent neoplasm. A focal area of increased uptake in the left upper quadrant (yellow arrows), consistent with a gastrojejunostomy tube. A second focus of radiotracer uptake is identified in the abdomen within the gastrojejunostomy tube (yellow arrows), external to the patient.

identified. The specimen cells demonstrated strong nuclear immunoreactivity for thyroid transcription factor 1 (TTF1) and variable cytoplasmic staining with thyroglobulin. Given the specimen characteristic nuclear features and immunophenotypic profile, the overall findings were consistent with a metastatic papillary thyroid carcinoma. All resection margins and peripancreatic lymph nodes were negative for carcinoma (Figure 7).

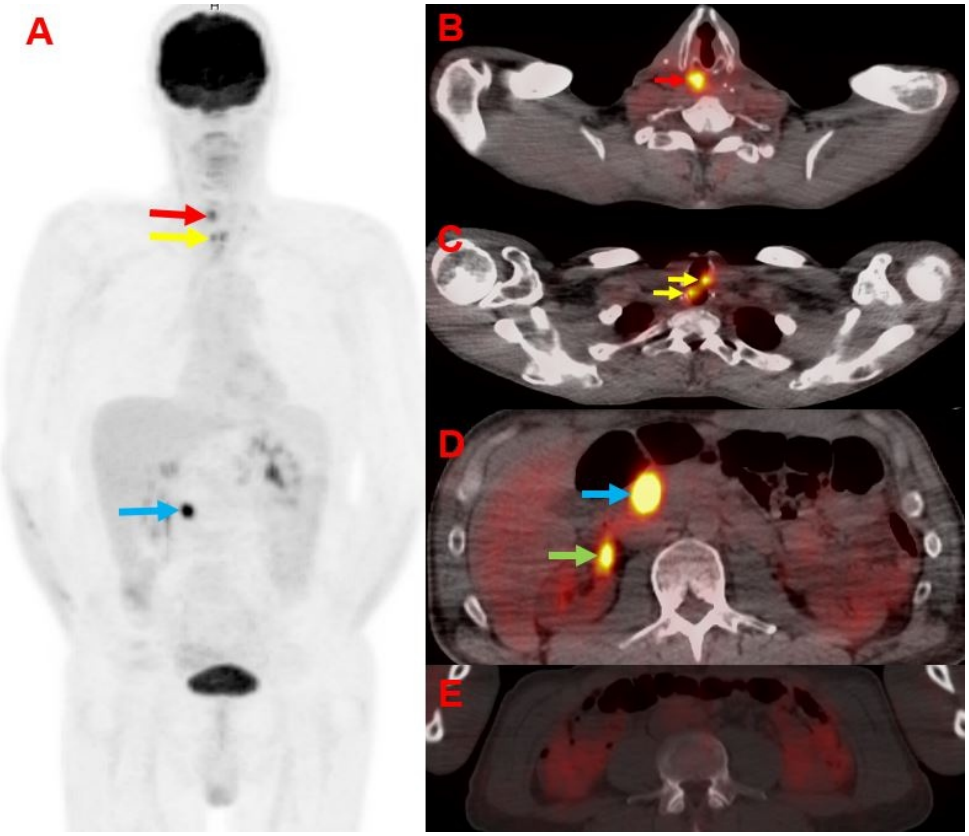

Figure 6. (A) Fluorine-18-FDG-PET/CT maximum intensity projection (MIP) from skull base to mid-thigh and (B-E) axial fused ^{18}F-FDG PET/CT images demonstrate a focal area of asymmetric increased ^{18}F-FDG uptake in the region of the right vocal cord related to compensatory muscle activity secondary to left vocal cord paralysis (red arrows), recurrent thyroid neoplasm (yellow arrows), metastases to the pancreatic head (blue arrows) and physiologic ^{18}F-FDG uptake within the right renal collecting system (green arrow). There is no abnormal ^{18}F-FDG uptake within the L4 vertebra at this time, opposed to suspicious osseous metastasis shown on a subsequent surveillance ^{18}F-FDG PET/CT examination (see Figure 8).

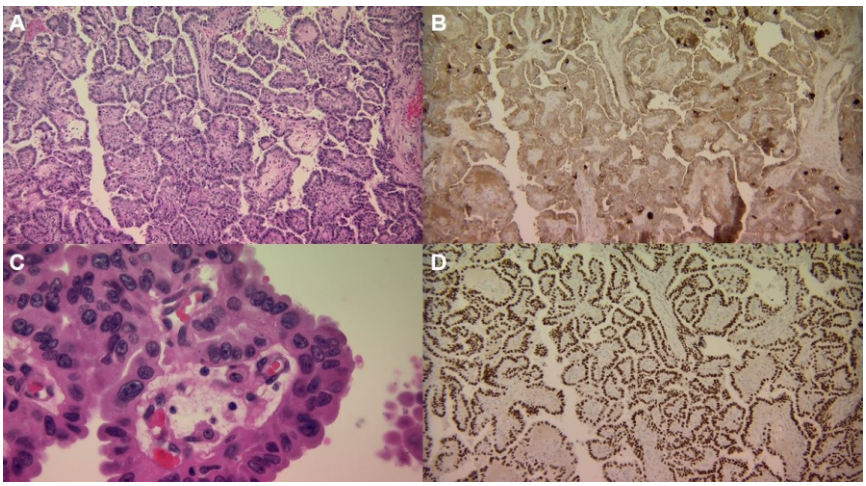

Figure 7. (A) A low-power hematoxylin-eosin preparation at x100 magnification of the resected pancreatic head mass, demonstrates papillary architecture with fibrovascular cores. (B) Immunohistochemical preparation for thyroglobulin at x100 magnification demonstrates variable cytoplasmic staining in neoplastic cells. (C) Nuclear grooves, pseudoinclusions, and prominent nucleoli can be visualized on a high-power hematoxylin-eosin preparation at ×600 magnification. (D) The mass demonstrates strong and diffuse nuclear staining for TTF1 at x100 magnification. A combination of these findings on histopathological analysis is consistent with metastatic papillary thyroid carcinoma within the pancreatic head.

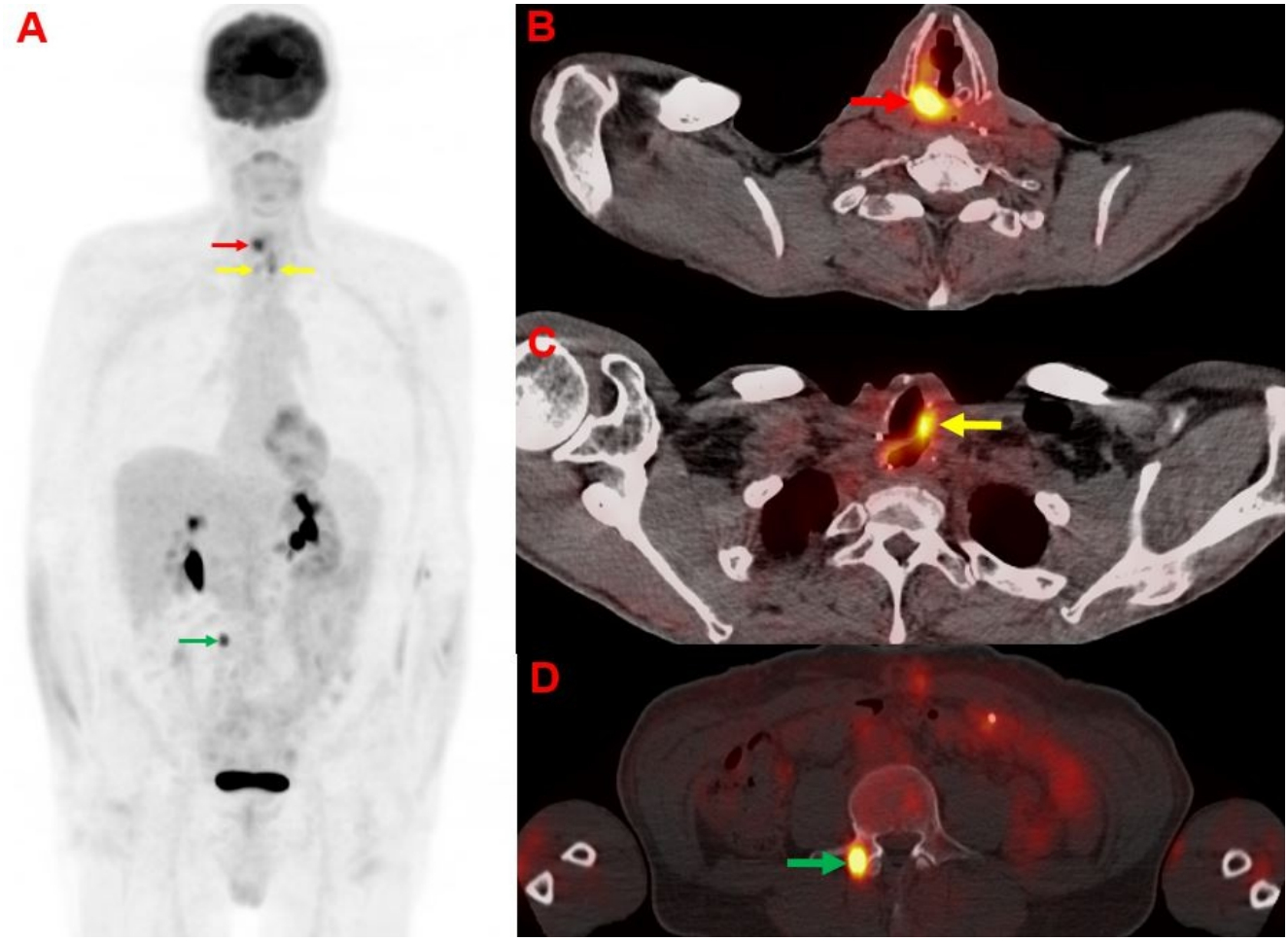

Figure 8. (A) Post-resection surveillance ^{18}F-FDG PET/CT MIP from the skull base to mid-thigh and (B-D) axial fused ^{18}F-FDG PET/CT images demonstrate a focal area of asymmetric increased ^{18}F-FDG uptake in the region of the right vocal cord related to compensatory muscle activity secondary to left vocal cord paralysis (red arrows), recurrent thyroid neoplasm (yellow arrows), and incurrent focal area of increased uptake at the L4 pedicle on the right, suspicious for osseous metastasis (green arrows).

The patient was started on post-surgical systemic chemotherapy, Lenvatinib. He was monitored for recurrent metastatic disease with routine surveillance ^{18}F-FDG PET/CT examinations every 6 months. An ^{18}F-FDG PET/CT performed 6 months after resection of the metastatic pancreatic papillary thyroid carcinoma demonstrated persistent residual/recurrent thyroid neoplasm, as seen on prior examinations. There were no recurrent ^{18}F-FDG avid lesions within the pancreatic resection bed or lesser sac; however, there was an incurrent ^{18}F-FDG avid lesion within the right L4 pedicle, suspicious for osseous metastasis (Figure 8).

Material and Methods

The literature was reviewed using PubMed and MEDLINE search engines. The search term "papillary thyroid carcinoma" was paired with phrases "pancreatic metastases" and "metastases to pancreas", which yielded 109 results. Sixteen of the 109 results revealed case reports of pancreatic metastases of PTC that were identified via the article title name and abstract. The 16 relevant abstracts and articles that included pathologically proven papillary thyroid carcinoma, and its variants, metastases to the pancreas were thoroughly examined. The references and tables of the 16 case reports were crosschecked to compile the list of all case reports of pancreatic metastasis from PTC reported. Of note, one article had two reported cases, therefore determining that there are 17 cases reported in the literature to date.

Discussion

Locoregional metastases of PTC to the cervical lymph nodes are significantly more common than distant metastases. Distant metastases are typically associated with the more aggressive variants of PTC such as tall cell; however, are still seen in the classical variant [9]. The BRAFV600E mutation has been linked with increased aggression and poor prognosis [13]. Patients with distant metastases outcomes are affected by age, metastatic tumor size and radio-iodine-sensitivity [9]. Standard treatment for PTC involves total thyroidectomy and RAI ablation. RAI ablation is still recommended as first line treatment for PTC metastases if they are radio-iodine-sensitive [16]. When thyroglobulin (TG) levels rise after RAI ablation, ^{18}F-FDG PET/CT scans are performed to assess for residual or recurrent lesions. Often times PTC metastases are detected on these scans as hypermetabolic lesions.

Pancreatic metastases from other primary sources are rare, occurring in only 2%-5% of cases [21]. The most common primary tumors that metastasize to the pancreas are kidney, lung, breast, colon, and skin cancers [21]. While there is no general imaging protocol for detection of pancreatic metastases, imaging recommendations follow those of the suspected primary lesion, but are usually diagnosed via routine follow up CT imaging [22]. Other imaging modalities such as dynamic contrast-enhanced CT imaging, magnetic resonance imaging (MRI), and endoscopic ultrasound (EUS) may be used [22]. Endoscopic ultrasound with biopsy can play a fundamental role in the tissue diagnosis of pancreatic metastases[18].

Including our case there are 18 reported cases in the literature to date with important distinctions, in regards to imaging, summarized in Table 1 [3-19]. Therefore, pancreatic metastases from PTC are very rare. Normally, pancreatic metasases are incidentally found given the anatomical location of the pancreas causing symptomatology to occur in late stage disease. Ren et al. (2020), described the only case where the pancreatic metastases was the initial presentation subsequently leading to discovery of the primary PTC [7]. Papillary thyroid carcinoma was demonstrated to metastasize to the pancreas as early as 2 to 15 years from the initial diagnosis. The average age was 67 years old and was male predominate in 13 of the 18 cases. The pancreatic metastasis was found in the head of the pancreas in 9 of the cases making that the most common anatomic location for metastases observed. In our literature review, size of the metastases ranged from 0.8cm to 8.5cm.

Typically pancreatic lesions are solid lesions with well-defined borders in comparison to irregular margins associated with primary pancreatic lesions [22]. Triantopoulou et al. (2012), first observed that the "duct penetrating sign", where the pancreatic duct is continuous throughout the lesion, may be a distinguishing feature of pancreatic metastases over primary pancreatic tumors as metastatic lesions tend to compress the duct rather than invade and disrupt the ductal architecture [22]. Both of these distinguishing features where were highlighted in our review with 13 cases describing or revealing well-circumscribed lesions in the images associated with their report. Angeles et al. (2009) and Meyer et al. (2006), respectively reported a non-encapsulated and encapsulated, well-defined surgical specimens, which coincide with the image findings [10, 16]. In various imaging modalities pancreatic metastases appear hypoechoic on ultrasound (US), hypodense on CT, hypointense on T1-weighted MR images, heterogenous intermediate to hyperintense on T2-weighted MR images, and enhance on contrasted CT and MRI images, as highlighted in Table 1 [22].

For our patient, the dose of RAI was determined based on the recommendations from The Society of Nuclear Medicine & Molecular Imaging Practice Guideline for Therapy of Thyroid Disease with ^{131}I 3.0 which states, "the greater the risk of metastases or recurrent tumor and the more extensive the invasiveness or dissemination of the cancer at the time of therapy, the higher the ^{131}I activity required" [23]. Given these recommendations, our patient was in the high risk category based on tumor invasion within the left recurrent laryngeal nerve, trachea, and esophagus, incomplete surgical removal of the neoplasm, involvement of the cervical lymph nodes, unfavorable tall cell variant of papillary thyroid carcinoma, and very high thyroglobulin level in absence of elevated thyroglobulin antibodies level. Therefore, our patient received 200mCi ^{131}I to eliminate as much known residual neoplasm as possible and eradicate likely microscopic metastasis.

All but 2 cases reported patients receiving RAI ablation therapy and 2 additional cases did not comment on RAI ablation therapy. Interestingly, our case received 2 rounds of RAI ablation prior to detection of his pancreatic metastases and 8 of the 18 cases also reported multiple treatments of RAI ablation prior to metastatic detection. Also of recognition, 8 of the 18 cases underwent ^{131}I whole body scintigraphy showing non-avidity, revealing the metastases failure to uptake iodine. Conversely, 9 of the 18 cases were detected on ^{18}F-FDG PET/CT revealing a hypermetabolic lesion in 8 of those cases.

Fluorine-18-FDG PET/CT scan can detect localized PTC metastases that are negative on ^{131}I whole-body scans with high accuracy, but no data currently exists on its accuracy for distant metastases [24]. This discrepancy may be explained by metastatic PTC having different iodide symporter gene expression opening up the propensity to metastasize, lack of PTC pancreatic metastases avidity to iodine, and ability to uptake RAI [4, 13]. Recently, Wong et al. (2021) demonstrated that ^{124}I PET/CT, a new diagnostic imaging modality, may be used for detection and dosimetry for RAI treatment of PTC pancreatic metastases.

In conclusion, pancreatic metastases in patients with PTC are extremely rare. PTC most commonly metastasizes to the head of the pancreas anywhere from 2-15 years after initial diagnosis. Specific imaging criteria is a diagnostic dilemma given the variability in presentation and time interval until pancreatic metastases occur; however, rising TG levels post-RAI ablation should warrant additional ^{18}F-FDG PET/CT scans to assess for pancreatic metastases. PTC pancreatic metastases may go unrecognized under whole body ^{123}Iscans as they are often not radio-iodineavid. New modalities such as ^{124}I PET/CT may allow for better detection of PTC pancreatic metastases.

Table 1. *Summary of PTC pancreatic metastases cases.*

Author	Year	Age	Gender	Histology	RAI	Imaging Modality	Iodine avid	Imaging Characteristics	Location in Pancreas	Yrs from initial diagnosis
Present Case	2021	46	M	TCPTC	Yes x2	^{18}F-FDG PET/CT	No	3 cm well-circumscribed hypermetabolic	Head	3
Wong	2021	75	M	PTC	Yes x3	^{124}I-PET/CT	Yes	hypodense, well-circumscribed lesion w/ atrophy of distal pancreas hypermetabolic	Body and Tail	7
Tramontin	2020	73	M	PTC	Yes	^{18}F-FDG PET	n/a	2.8 cm mass	Head	6
Rossi	2020	60	M	PTC	No	CT/MRI/EUS	n/a	2 cm hypoechoic lesion and intraductal growth	Head	15
Ren	202	47	M	PTC	Yes	US/CT	n/a	4 cm x 3 cm pancreatic space occupying lesions with main ductal dilation	Body and Tail	0
Cho	2017	81	M	PTC	Yes	Abdominal MRI ^{18}F-FDG PET/CT MRI cholangiogram	n/a	non-enhancing cystic lesion, no ductal dilation hypermetabolic lesion 1 cm x 0.8 cm T1 hypointense, slightly T2 hyperintense, diffusion restriction, peripheral enhancement	Head/Body	10
Davidson	2017	84	F	TCPTC	Yes	^{18}F-FDG PET CT w/wo	n/a	hypermetabolic, well-circumscribed 1.1 cm enhancing mass	Body	2
Li	2014	66	M	PTC	n/a	CT w/wo ^{18}F-FDG PET	n/a	6.2 cm x 5.8 cm heterogenously enhancing mass with clear border hypometabolic	Body and Tail	11

(continued)

Tunio	2013	67	F	FVPTC	Yes x2	CT w/wo MRCP	No	decreased enhancement of neck/body/tail, normal enhancement of head 1.8 cm x 1. 5cm hypovascular lesions, T1 and T2 hypointense, faint enhancement, well-circumscribed	Neck	7
Alzahrani	2012	55	M	PTC	Yes x2	^{18}F-FDG PET/CT MRI	No	1.7 cm well-circumscribed hypermetabolic	Head	8
Chen	2010	82	M	PTC	Yes	EUS	n/a	n/a	Neck	5
Borschitz (1)	2010	44	F	FVPTC	Yes x3	^{18}F-FDG PET/CT MRI	No	light pathological enhancement hypermetabolic, T1 hypointense, T2 intermediate well-circumscribed	Head	10
Borschitz (2)	2010	61	M	PTC	Yes x2	^{18}F-FDG PET/CT MRI	No	hypermetabolic isodense well-circumscribed lesion	Body	15
Angeles	2009	72	M	PTC	n/a	CT	n/a	8.5 cm nonecapsulated, well-circumscribed (surgical specimen)	Body and Tail	n/a
Siddiqui	2006	67	M	TCPTC	Yesx2	^{18}F-FDG PET/CT EUS	No	Hypermetabolic, hypodense mass 1.5 cmx1.1 cm well-defined hypoechoic, homogenous mass	Head	7
Meyer	2006	67	M	PTC	Yes	Blood pool scintingraphy CT	No	capsule (surgical specimen)	Head	5
Jobran	2000	53	M	TCPTC	Yes x2	MRI	No	3 cm x 4 cm, well-circumscribed	Head	1
Sugimura	1991	39	F	PTC	No	ERCP CT w/wo	n/a	hypervascular on arteriography 5 cm isodense lesion w/ clear margin, enhancing	Head	7

YRS = years, RAI = radioactive iodine ablation, PTC = papillary thyroid cancer, TCPTC = tall cell papillary thyroid cancer, FVPTC = follicular variant papillary thyroid cancer, n/a = not available, 18F-FDG PET/CT = fluorine-18-fluorodeoxyglucose positron emission tomography/computed tomography, 124I = iodine-124, CT = computed tomography, MRI = magnetic resonance imaging, EUS = endoscopic ultrasound, w/wo: with and without IV contrast.

Bibliography

1. Cipriani NA. Prognostic Parameters in Differentiated Thyroid Carcinomas. *Surg Pathol Clin* 2019; 12:883-900.
2. Surveillance, Epidemiology, and End Results Program Cancer Stat Facts. Thyroid Cancer National Cancer Institute, DCCPS, Surveillance Research Program; 2016. Date Accessed: March 10, 2021. https://seer.cancer.gov/statfacts/html/thyro.html
3. Nath MC, Erickson LA. Aggressive Variants of Papillary Thyroid Carcinoma: Hobnail, Tall Cell, Columnar, and Solid. *Adv Anat Pathol* 2018; 25: 172-9.
4. Cho M, Acosta-Gonzalez G, Brandler TC et al. Papillary thyroid carcinoma metastatic to the pancreas: Case report. *Diagn Cytopathol* 2019; 47: 214-7.
5. See A, Iyer NG, Tan NC et al. Distant metastasis as the sole initial manifestation of well-differentiated thyroid carcinoma. *Eur Arch Otorhinolaryngol* 2017; 274: 2877-82.
6. Tunio MA, AlAsiri M, Riaz K, AlShakweer W. Pancreas as Delayed Site of Metastasis from Papillary Thyroid Carcinoma. *Case Rep Gastrointest Med* 2013; 2013: 386263.
7. Ren H, Ke N, Tan C et al. Unusual metastasis of papillary thyroid cancer to the pancreas, liver, and diaphragm: a case report with review of literature. *BMC Surgery* 2020; 20: 82.
8. Sugimura H, Tamura S, Kodama T et al. Metastatic pancreas cancer from the thyroid; clinical imaging mimicking non functioning islet cell tumor. Radiat Med 1991; 9:167-9.
9. Jobran R, Baloch ZW, Aviles V et al. Tall cell papillary carcinoma of the thyroid: metastatic to the pancreas. *Thyroid* 2000; 10: 185-7.
10. Angeles-Angeles A, Chable-Montero F, Martinez-Benitez B, Albores-Saavedra J. Unusual metastases of papillary thyroid carcinoma: report of 2 cases. *Ann Diagn Pathol* 2009; 13: 189-96.
11. Borschitz T, Eichhorn W, Fottner C et al. Diagnosis and treatment of pancreatic metastases of a papillary thyroid carcinoma. *Thyroid* 2010; 20:93-8.
12. Chen L, Brainard JA. Pancreatic metastasis from papillary thyroid carcinoma diagnosed by endoscopic ultrasound-guided fine needle aspiration: a case report. *Acta Cytol* 2010; 54: 640-4.
13. Alzahrani AS, AlQaraawi A, Al Sohaibani F et al. Pancreatic metastasis arising from a BRAF(V600E)-positive papillary thyroid cancer: the role of endoscopic ultrasound-guided biopsy and response to sorafenib therapy. *Thyroid* 2012; 22: 536-41.
14. Siddiqui AA, Olansky L, Sawh RN, Tierney WM. Pancreatic metastasis of tall cell variant of papillary thyroid carcinoma: diagnosis by endoscopic ultrasound-guided fine needle aspiration. *JOP* 2006; 7: 417-22.
15. Li XO, Li ZP, Wang P et al. Pancreatic metastasis of papillary thyroid carcinoma: a case report with review of the literature. *Int J Clin Exp Pathol* 2014; 7: 819-22.
16. Meyer A, Behrend M: Is pancreatic resection justified for metastasis of papillary thyroid cancer? *Anticancer Res* 2006, 26: 2269-73.
17. Davidson M, Olsen RJ, Ewton AA, Robbins RJ. Pancreas Metastases from Papillary Thyroid Carcinoma: A Review of the Literature. *EndocrPract* 2017; 23:1425-9.
18. Rossi G, Petrone MC, Schiavo Lena M et al. Pancreatic metastasis of papillary thyroid carcinoma with an intraductal growth pattern. *Endoscopy* 2020; 52: E452-e3.
19. Tramontin MY, Faria PAS, Nascimento CMD et al.Cholestatic syndrome as initial manifestation of pancreatic metastasis of papillary thyroid carcinoma: case report and review. *Arch Endocrinol Metab* 2020; 64: 179-84.
20. Wong BZY, Dickie G, Garcia P et al.^{124}I-PET/CT-Guided Diagnosis and Personalized Treatment of Metastatic Papillary Thyroid Cancer to the Pancreas. *Clin Nucl Med* 2021; 46(4): 337-9.
21. Pang JC, Roh MH. Metastases to the Pancreas Encountered on Endoscopic Ultrasound-Guided, Fine-Needle Aspiration. *Arch Pathol Lab Med* 2015; 139: 1248-52.
22. Triantopoulou C, Kolliakou E, Karoumpalis I et al. Metastatic disease to the pancreas: an imaging challenge. *Insights Imaging* 2012; 3: 165-72.
23. Silberstein EB, Alavi A, Balon HR et al. The SNMMI practice guideline for therapy of thyroid disease with ^{131}I 3.0. *J Nucl Med* 2012; 53: 1633-51.
24. Chung JK, So Y, Lee JS et al. Value of FDG PET in papillary thyroid carcinoma with negative ^{131}I whole-body scan. *J Nucl Med* 1999; 40:986-92.